Electronic Supplementary Information

Mesoporous polyacrylic acid/calcium phosphate coated persistent luminescence nanoparticles for improved afterglow bioimaging and chemotherapy of bacterial infection

Xuan Fu,[abc] Xu Zhao,[abc] Li-Jian Chen,[abc] Pi-ming Ma,[d] Tianxi Liu,[de] and Xiu-Ping Yan [*abcd]

[a] State Key Laboratory of Food Science and Technology, Jiangnan University, Wuxi, 214122, China

[b] International Joint Laboratory on Food Safety, Jiangnan University, Wuxi 214122, China

[c] Institute of Analytical Food Safety, School of Food Science and Technology, Jiangnan University, Wuxi, 214122, China

[d] Key Laboratory of Synthetic and Biological Colloids, Ministry of Education, Jiangnan University, Wuxi, 214122, China

[e] School of Chemical and Material Engineering, International Joint Research Laboratory for Nano Energy Composites, Jiangnan University, Wuxi 214122, China

[*] Corresponding author

E-mail address: xpyan@jiangnan.edu.cn

Supplementary Figures

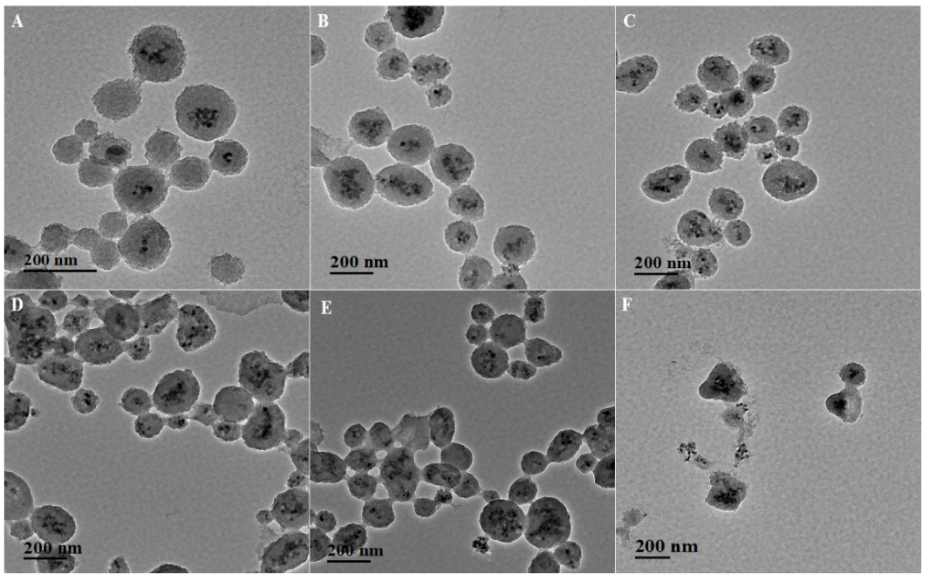

Fig. S1 TEM images of PLNPs@PAA/CaP prepared with (A) 30, (B) 40, (C) 50, (D) 60, (E) 75, and (F) 100 mg of PLNPs.

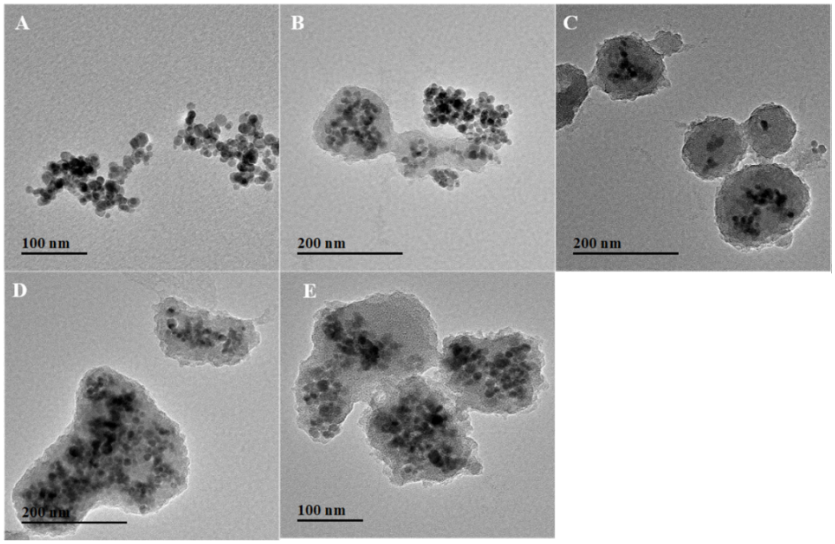

Fig. S2 TEM images of PLNPs@PAA/CaP prepared with (A) 90, (B) 110, (C) 130, (D) 150, (E) 170 mg of $Ca(OH)_2$.

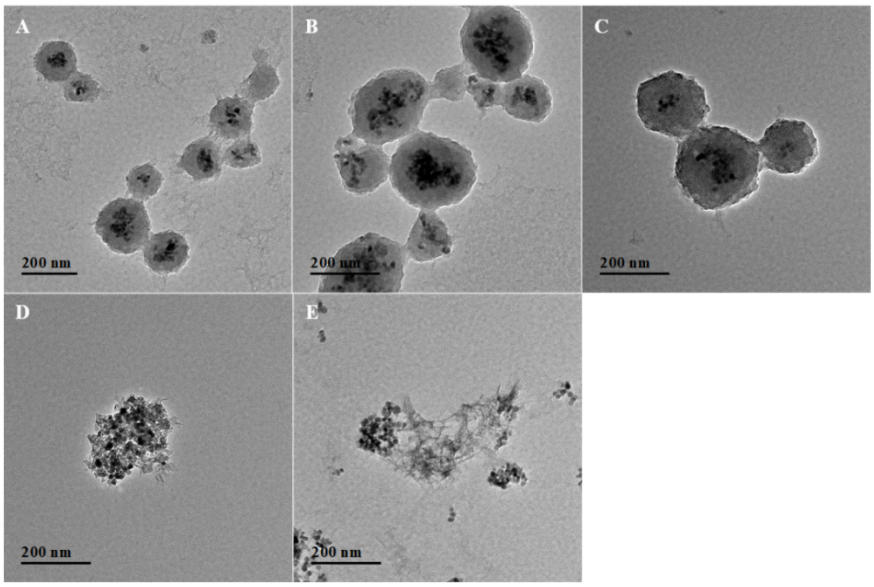

Fig. S3 TEM images of PLNPs@PAA/CaP prepared with (A) 100, (B) 125, (C) 150, (D) 300, (E) 450 mL of IPA.

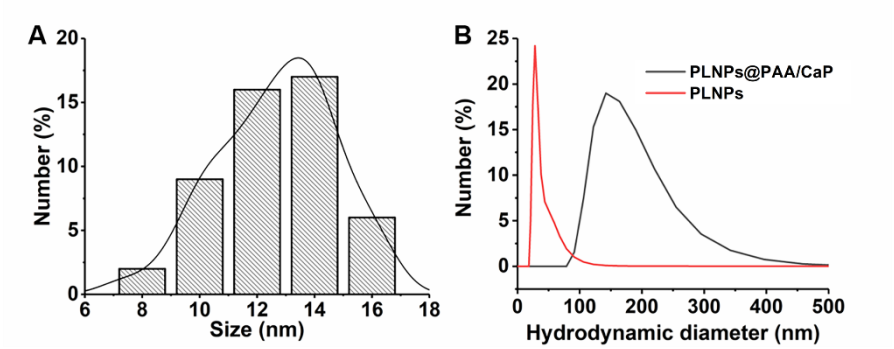

Fig. S4 (A) Size distribution of PLNPs based on 100 randomly selected nanoparticles. (B) Hydrodynamic diameter of PLNPs and PLNPs@PAA/CaP in PBS (10 mM, pH 7.4).

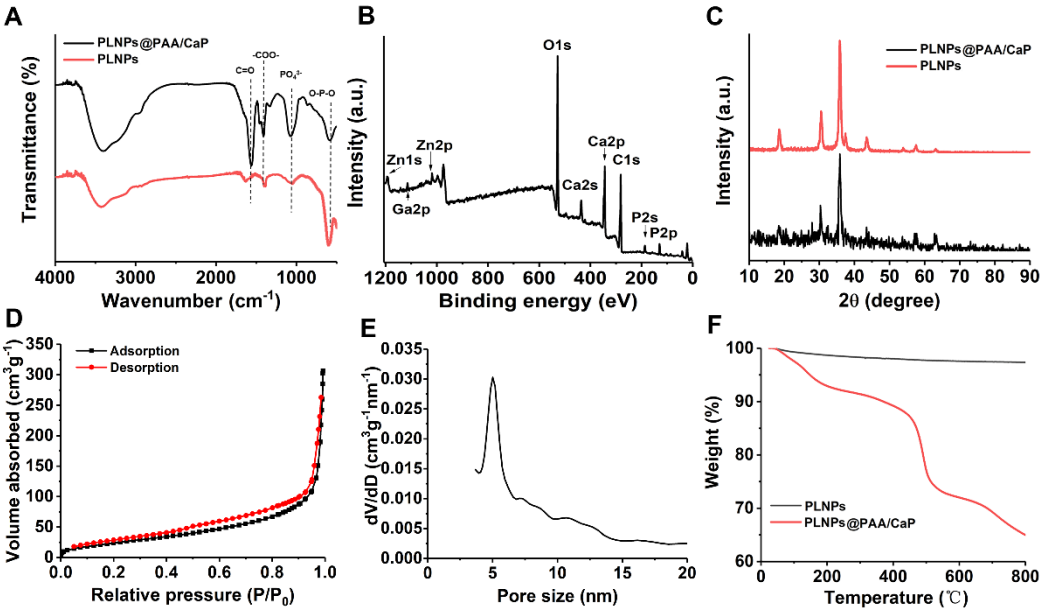

Fig. S5 (A) FT-IR spectra of PLNPs and PLNPs@PAA/CaP; (B) XPS spectra of PLNPs and PLNPs@PAA/CaP; (C) XRD patterns of PLNPs and PLNPs@PAA/CaP; (D) N_2 absorption-desorption isotherm of PLNPs@PAA/CaP; (E) Pore-size distribution of PLNPs@PAA/CaP; (F) TGA curves of PLNPs, and PLNPs@PAA/CaP.

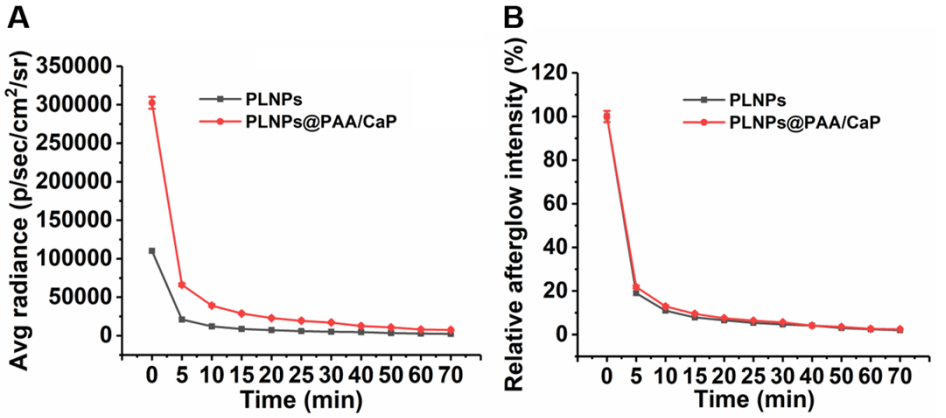

Fig. S6 (A) Change of afterglow intensity with time for PLNPs and PLNPs@PAA/CaP (LED 2 min); (B) Change of normalized relative afterglow intensity with time for PLNPs and PLNPs@PAA/CaP(LED 2 min).

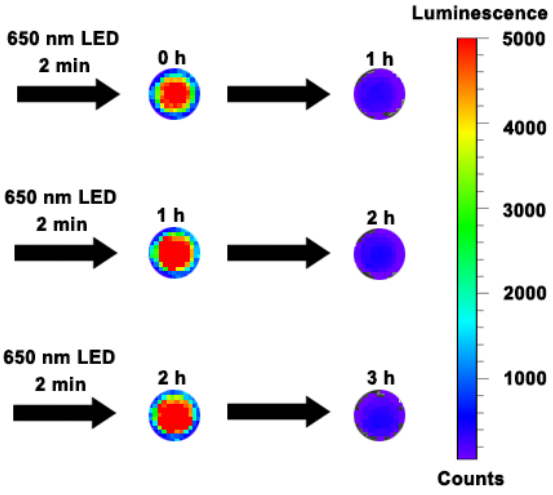

Fig. S7 Afterglow imaging of PLNPs@PAA/CaP (1 mg mL^{-1} in pH 7.4 PBS). PLNPs@PAA/CaP was repeatedly excited by 650 nm LED light for 2 min three times, then the persistent luminescence images were recorded.

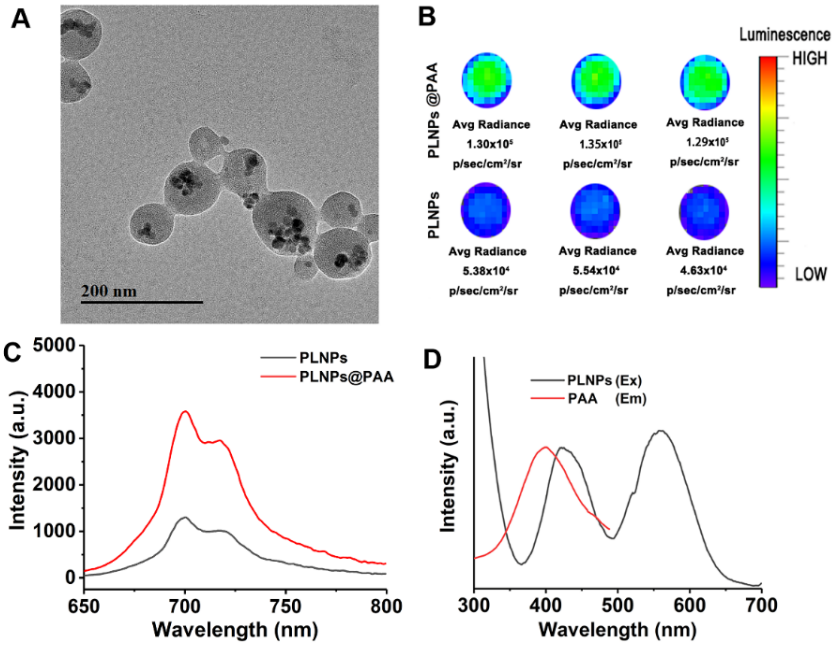

Fig. S8 (A) TEM image of PLNPs@PAA. (B) Afterglow images of PLNPs and PLNPs@PAA (254 nm UV irradiation for 5 min). (C) Luminescence intensity of PLNPs (0.1mg mL^{-1}) and PLNPs@PAA (0.1 mg mL^{-1} as PLNPs). (D) Emission spectra of PAA (ex: 254 nm) and excitation spectra of PLNPs in water

(em: 700 nm).

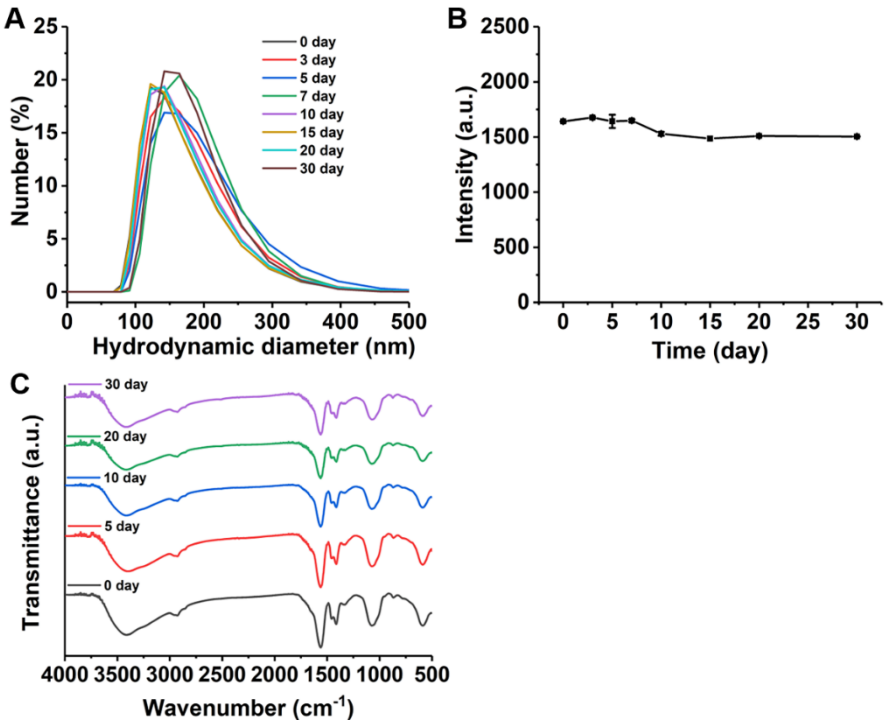

Fig. S9 (A) Time-dependent hydrodynamic diameter of PLNPs@PAA/CaP in pH 7.4 PBS (10 mM). (B) Time-dependent phosphorescence intensity of PLNPs@PAA/CaP in pH 7.4 PBS (10 mM). (C) Time-dependent FT-IR spectra of PLNPs@PAA/CaP in pH 7.4 PBS (10 mM).

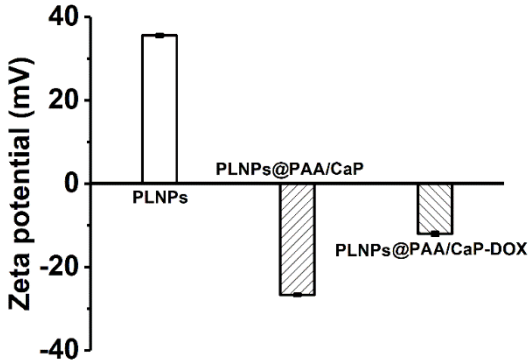

Fig. S10 Zeta potential of PLNPs, PLNPs@PAA/CaP, and PLNPs@PAA/CaP-DOX.

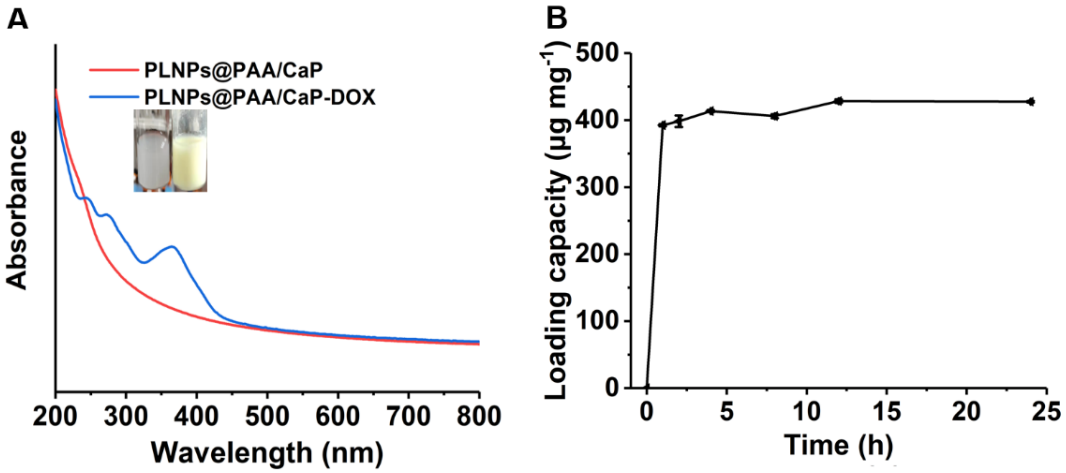

Fig. S11 (A) UV-vis absorption spectra of PLNPs@PAA/CaP and PLNPs@PAA-DOX (insert: photograph of PLNPs@PAA/CaP and PLNPs@PAA/CaP-DOX). (B) Effect of loading time on drug loading capacity.

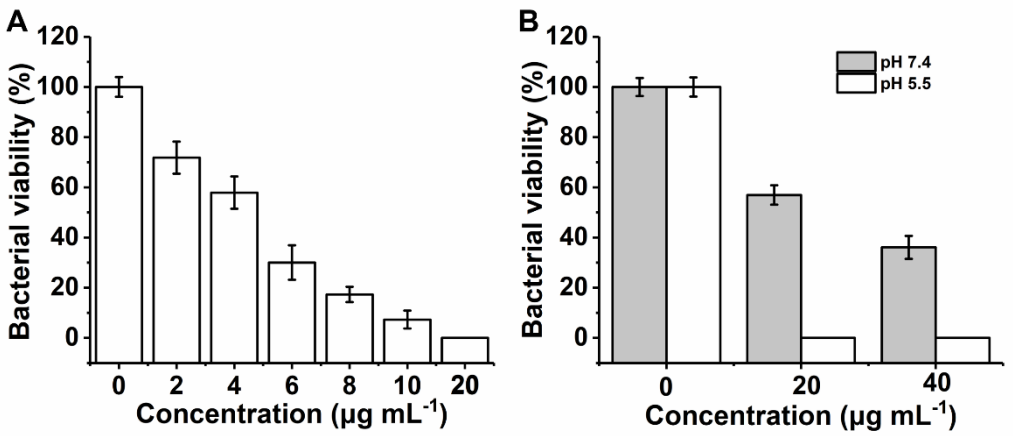

Fig. S12 (A) Viability of MRSA incubated with PLNP@PAA/CAP-DOX at various concentrations (pH 5.5). (B) Bacterial viability of MRSA incubated with PLNP@PAA/CAP-DOX at various concentrations (pH 7.4 and pH 5.5). The average number of colonies in the blank group with pH 5.5 was 135, and that in the blank group with pH 7.4 was 150. The results show that the viability of MRSA in the control group at pH 7.4 and 5.5 is similar.

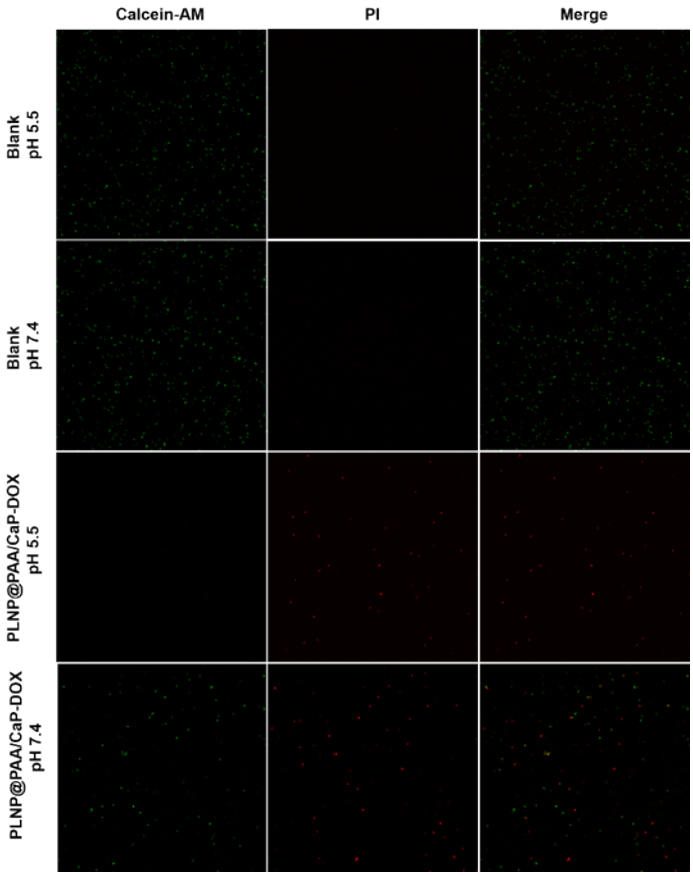

Fig. S13 Live/dead fluorescent bacterial staining treated with PBS and PLNP@PAA/CAP-DOX (20 μg mL^{-1}) at different pH values (pH 5.5 and pH 7.4).

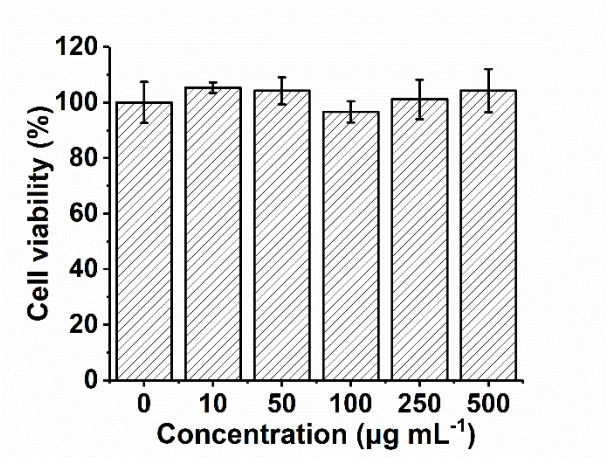

Fig. S14 Cell viability of 3T3 cells incubated with PLNPs@PAA/CaP at various concentrations for 24 h. Data were presented as the mean ± SD (*n* = 3).

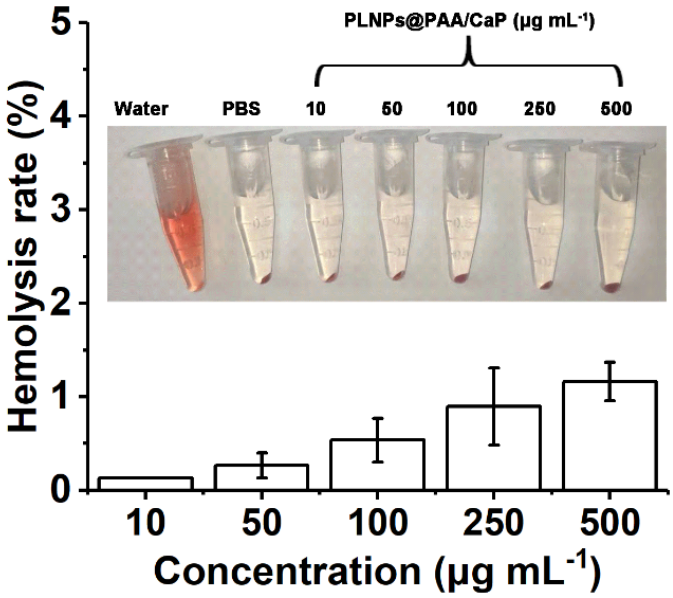

Fig. S15 Hemolysis rate of red blood cells incubated with various concentrations of PLNPs@PAA/CaP. The insert shows the corresponding photos of red blood cells with different treatments. Data were presented as the mean ± SD (*n = 3*).

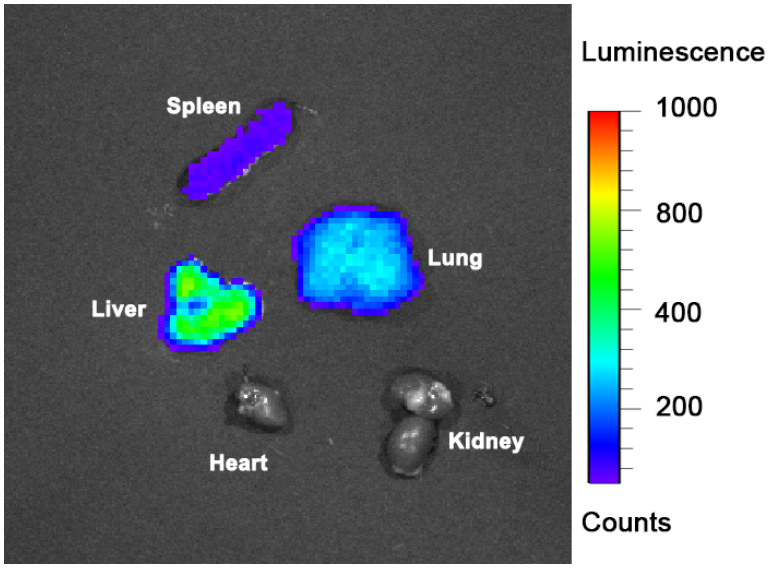

Fig. S16 Afterglow image of major organs for the mice at 24 h after PLNPs@PAA/CaP-DOX injection.

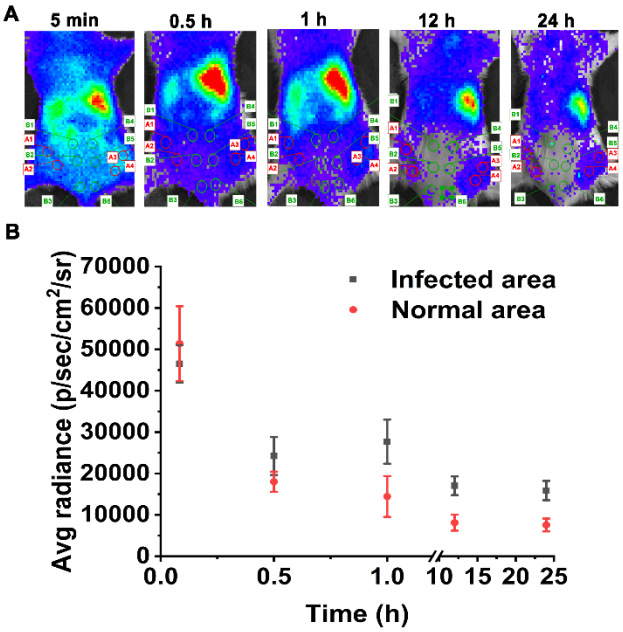

Fig. S17 (A) Selection of infected area and normal area (red cycle: infected area; green cycle: normal area). (B) Comparison of afterglow intensity between infected area and normal area. The results show that PLNP@PAA/CaP-DOX can be accumulated in the infected area.

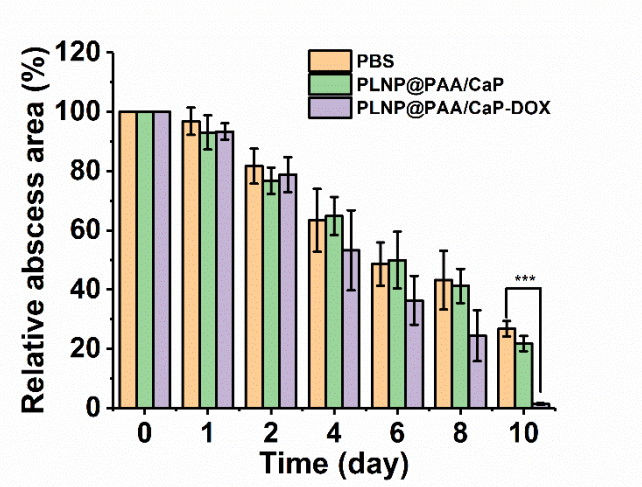

Fig. S18 Evaluation of the relative infected wound area over time. Data were presented as mean ± SD (*n* = *5*). *p < 0.001.

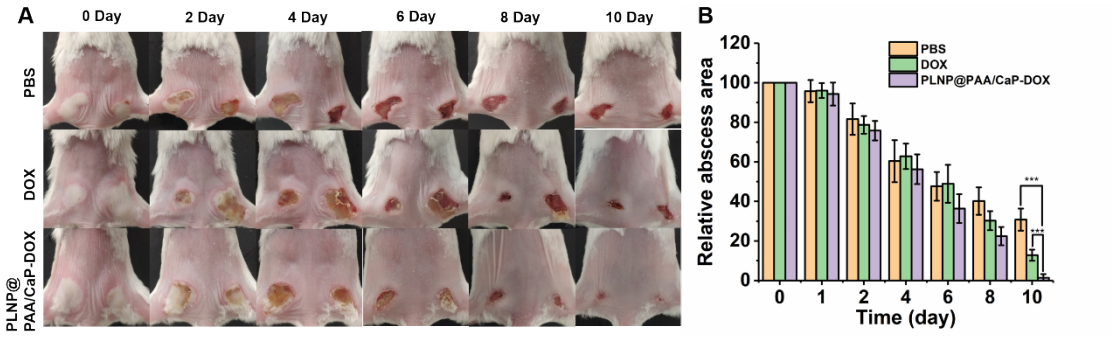

Fig. S19 (A) Photographs of MRSA-infected mice after different treatments (PBS, DOX and PLNPs@PAA/CaP-DOX) for 0, 2, 4, 6, 8, and 10 days; (B) Evaluation of the relative infected wound area over time. Data were presented as mean ± SD (*n* = *5*). *p < 0.001.

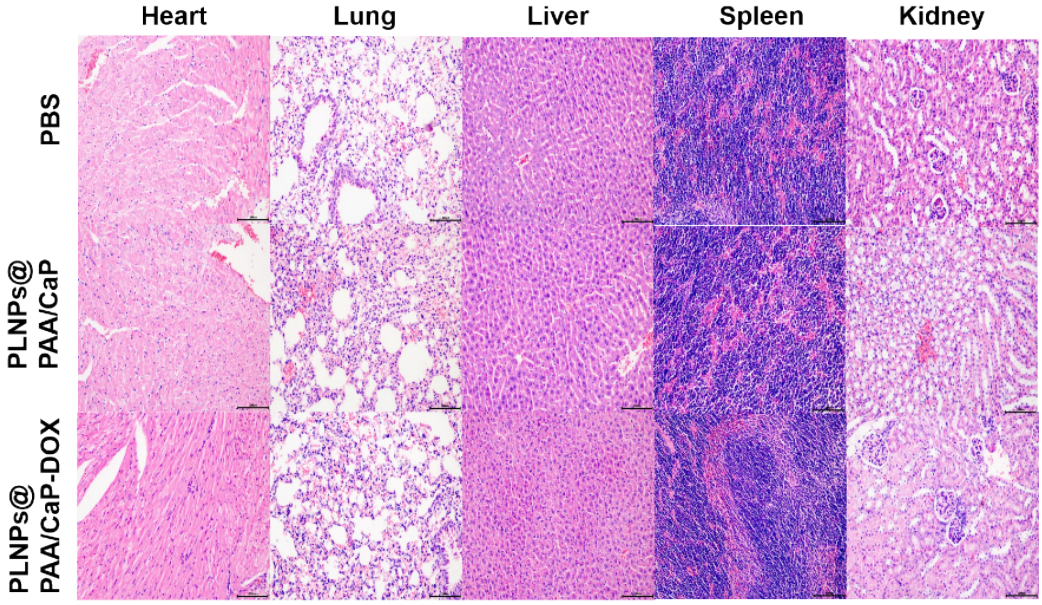

Fig. S20 H&E staining images of major organs of mice after different treatments (PBS, PLNPs@PAA/CaP, and PLNPs@PAA/CaP-DOX). Scale bar is 100 μm.

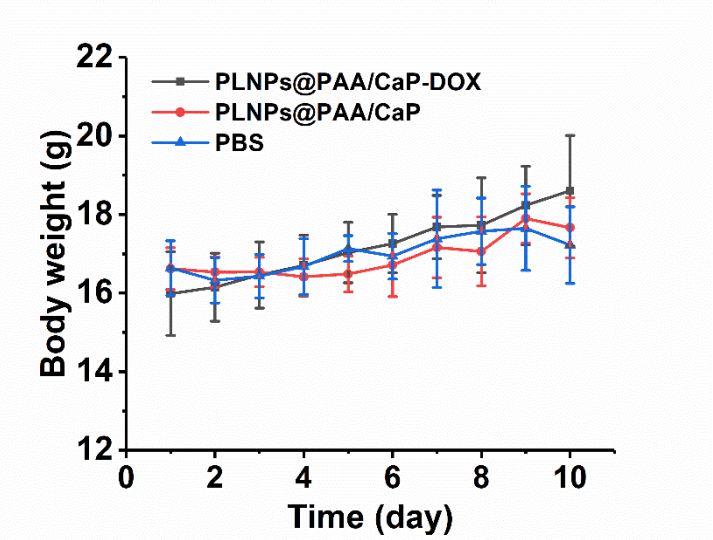

Fig. S21 Body weight variation among infected mice within 10 days after different treatments (PBS, PLNPs@PAA/CaP, and PLNPs@PAA/CaP-DOX).